Host cytoskeletal vimentin serves as a structural organizer and an RNA-binding protein regulator to facilitate Zika viral replication

Yue Zhang[a,b], Shuangshuang Zhao[c,d], Yian Li[b,e], Fengping Feng[f], Min Li[g], Yanhong Xue[f], Jie Cui[b,e], Tao Xu[f], Xia Jin[g,1], and Yaming Jiu[a,b,c,d,1]

[a]The Center for Microbes, Development and Health, Key Laboratory of Molecular Virology and Immunology, Institut Pasteur of Shanghai, Chinese Academy of Sciences, Shanghai 200031, China; [b]University of Chinese Academy of Sciences, Beijing 100049, China; [c]The Joint Program in Infection and Immunity, Guangzhou Women and Children's Medical Center, Guangzhou Medical University, Guangzhou 510623, China; [d]The Joint Program in Infection and Immunity, Institut Pasteur of Shanghai, Chinese Academy of Sciences, Shanghai 200031, China; [e]Key Laboratory of Molecular Virology and Immunology, Institut Pasteur of Shanghai, Chinese Academy of Sciences, Shanghai 200031, China; [f]Institute of Biophysics, Chinese Academy of Sciences, Beijing 100101, China; and [g]Shanghai Public Health Clinical Center, Fudan University, Shanghai 201508, China

Edited by Jennifer Lippincott-Schwartz, Janelia Farm Research Campus, Ashburn, VA; received August 17, 2021; accepted January 4, 2022

Emerging microbe infections, such as Zika virus (ZIKV), pose an increasing threat to human health. Investigations on ZIKV replication have revealed the construction of replication complexes (RCs), but the role of cytoskeleton in this process is largely unknown. Here, we investigated the function of cytoskeletal intermediate filament protein vimentin in the life cycle of ZIKV infection. Using advanced imaging techniques, we uncovered that vimentin filaments undergo drastic reorganization upon viral protein synthesis to form a perinuclear cage-like structure that embraces and concentrates RCs. Genetic removal of vimentin markedly disrupted the integrity of RCs and resulted in fragmented subcellular dispersion of viral proteins. This led to reduced viral genome replication, viral protein production, and release of infectious virions, without interrupting viral binding and entry. Furthermore, mass spectrometry and RNA-sequencing screens identified interactions and interplay between vimentin and hundreds of endoplasmic reticulum (ER)-resident RNA-binding proteins. Among them, the cytoplasmic-region of ribosome receptor binding protein 1, an ER transmembrane protein that directly binds viral RNA, interacted with and was regulated by vimentin, resulting in modulation of ZIKV replication. Together, the data in our work reveal a dual role for vimentin as a structural element for RC integrity and as an RNA-binding-regulating hub during ZIKV infection, thus unveiling a layer of interplay between Zika virus and host cell.

intermediate filaments | vimentin | Zika virus | replication complexes | RNA-binding protein

Zika virus (ZIKV), a mosquito-borne enveloped RNA virus that belongs to the Flaviviridae family, has gained notoriety recently, due to its explosive outbreaks and association with serious clinical diseases, such as Guillain-Barré syndrome in adults and microcephaly in newborns (1–4). Currently, no ZIKV-specific therapies or prophylactic vaccines are available (5). ZIKV genome is a positive-sense, single-stranded RNA [ssRNA(+)] (6). The viral replication occurs on the surface of the endoplasmic reticulum (ER), where the double-strand RNA (dsRNA) is synthesized from viral genomic ssRNA(+) and transcribed into new proteins (7, 8). The viral genome is translated into a polyprotein, which is proteolytically processed into three structural proteins (capsid [C], precursor membrane [prM], and envelop [Env]) and seven nonstructural proteins (NS1, NS2A, NS2B, NS3, NS4A, NS4B, and NS5), by both host and viral proteases (9, 10). ZIKV infection can rewire cellular components to establish viral replication complexes (RCs), which increase the local concentration of viral and cellular factors for efficient viral replication (11–13). However, the function of rewired cytoskeleton network remains elusive in ZIKV infection.

Vimentin is the most abundant intermediate filaments (IFs), which generally surrounds the nucleus and extends throughout the cytoplasm, providing help to important biological processes, such as organelle positioning, cell migration, and cell signaling (14). Except for acting as an integrator of cellular mechanical functions, the highly dynamic nature of vimentin filaments enables it to respond rapidly to pathological stimuli (15). Several studies have observed the phenomenon of vimentin network rearrangement in viral infections and proposed that the role of intact vimentin scaffold could contribute to the viral life cycle (16–21). However, evidence for the dynamic changes of vimentin IFs during ZIKV infection and its contribution to RCs integrity and stability remain understudied.

In addition to providing a structural scaffold, there is evidence indicating that cytoskeletal proteins also regulate translational apparatus (22). For example, ribosomes can physically associate with microtubules (MTs) and F-actin in different cells (23, 24). Disorganization of F-actin by cytochalasin D impairs

Significance

We discovered a dual role of vimentin underlying Zika virus (ZIKV) replication. The vimentin network reorganizes to surround the replication complex. Depletion of vimentin resulted in drastic segregation of viral proteins and subsequent defective infection, indicating its function as an "organizer" that ensures the concentration of all necessary factors for high replication efficacy. With omics analysis, we prove that vimentin also functions as a "regulator" that dominates RNA-binding proteins during infection. These two roles complement one another to make an integrated view of vimentin in regulating ZIKV infection. Collectively, our study fills the long-term gap in our knowledge of the cellular function of intermediate filaments in addition to structural support and provides a potential target for ZIKV therapy.

Author contributions: Y.J. designed research; Y.Z., S.Z., Y.L., F.F., and Y.X. performed research; Y.L., M.L., and X.J. contributed new reagents/analytic tools; Y.Z., Y.L. and J.C. analyzed data; Y.J. and Y.Z. wrote the paper; and T.X. and X.J. edited versions of the manuscript.

The authors declare no competing interest.

This article is a PNAS Direct Submission.

[1]To whom correspondence may be addressed. Email: jinxia@shphc.org.cn or ymjiu@ips.ac.cn.

This article contains supporting information online at http://www.pnas.org/lookup/suppl/doi:10.1073/pnas.2113909119/-/DCSupplemental.

Published February 22, 2022.

local protein synthesis in isolated axoplasmic nerve fibers (25). The interaction between keratin IFs and the Y subunit of eukaryotic elongation factor-1 (eEF1BY) plays an essential role in protein synthesis (26). MTs can bind to the cytoplasmic tail of RRBP1 and take part in ER organization and neuronal polarity (27, 28). However, information on the spatial and functional relationship between vimentin IFs and the translational machinery, especially in the context of virus infection, remain completely unknown.

In this study, we investigated the function of vimentin IFs in ZIKV infection. By monitoring spatial-temporal responses of the cellular vimentin network throughout various steps of the ZIKV life cycle, we demonstrated that ZIKV infection induces massive rearrangements of cytoplasmic vimentin. When vimentin protein was genetically depleted from cells, distribution of viral proteins is scattered within infected cells, indicating its "organizer" role. Viral RNA replication, protein synthesis, and virion release are subsequently reduced. Using mass spectrometry (MS) and RNA-sequencing (RNA-seq) analysis, we discovered many intimate interactions between vimentin and RNA-binding proteins (RBPs), and that vimentin facilitates ZIKV RNA replication by interacting with and regulating the level and subcellular distribution of RRBP1, indicating its "regulator" role. Thus, our work establishes important connections among vimentin filaments dynamics, ZIKV RCs, and cellular RBPs in highly effective infection.

Results

ZIKV Infection Induces Drastic Cellular Vimentin Rearrangement and Formation of Cage-Like Structures. To study whether host cytoskeletal proteins respond to ZIKV infection, we examined the vimentin network using an established model with human osteosarcoma cells (U2OS) that express abundant cytoskeletal filaments and are highly susceptible to viruses (29–31) (Fig. 1 *A* and *D*). The cells were infected with an ZIKV Asian lineage strain, SZ01, and fixed at different time points (hours) postinfection (hpi). Viral nonstructural protein NS4B, which colocalized with structural protein envelop (Env) (*SI Appendix*, Fig. S1*A*) and endogenous vimentin, were visualized by immunofluorescence. In mock-infected cells, vimentin filaments showed perinuclear localization and radiated toward the cell periphery with apparent filamentous structure (Fig. 1*A*). However, the localization of vimentin rearranged markedly and formed compact aggregation together with viral protein near the nucleus, without any notable changes on cell size and overall morphology, within 48 hpi (Fig. 1 *A* and *B*).

A time-course study showed that viral RNA replication initiated from 8 hpi and reached to a plateau at 36 hpi and onward; concurrently, viral proteins start to synthetize from 12 hpi and become more pronounced afterward (Fig. 1 *C* and *D*). It was evident from the quantification that both viral RNA appearance and protein synthesis started before the virus-induced vimentin rearrangement, which was not yet initiated at 16 hpi. The vimentin compartments only appeared to shrink at around 24 hpi, and progressively reached a plateau at 36 hpi (Fig. 1 *B–D*). This suggests that vimentin concentration is not required to initiate virus replication. Instead, the emergence of viral proteins may act as a trigger for the vimentin rearrangements to occur. At the protein levels, however, cytoskeletal components—including actin, tubulin, and vimentin—were similar between ZIKV-infected and mock-infected cells throughout the infection lifecycle (Fig. 1*D*).

To describe the detailed dynamics of vimentin filament rearrangement, we generated a vimentin-mCherry stable-expression U2OS cell line and performed live-cell imaging analysis. A high multiplicity of infection (MOI) of input virus was used to achieve infection of every cell recorded. In mock-infected cells, no apparent changes of vimentin were observed within a 30-h monitoring period (Fig. 1*E*). In contrast, vimentin filaments gradually gathered around the nucleus from ∼20 hpi and progressively intensified in ZIKV-infected cells (Fig. 1*E* and Movies S1 and S2).

ZIKV multiplies in perinuclear RCs (32, 33). In order to gain insight into the spatial relationship between vimentin and viral protein, we took advantage of the three-dimensional–structured illumination microscopy (3D-SIM) for superresolution visualization. Side views of 3D images discovered that vimentin filaments form a hollow cage-like structure that wrap structural protein Env as well as nonstructural proteins NS1 and NS4B (Fig. 1*F* and *SI Appendix*, Fig. S2*D*). Furthermore, electronic microscopy elaborated events of enrichment of IF-like filaments next to the concentrated area of viral particles in the perinuclear region (Fig. 1*G* and *SI Appendix*, Fig. S2*E*). Together, these imaging observations indicated that ZIKV infection induced vimentin-cage formation around RCs.

Exogenous Expression of ZIKA Viral Protein Leads to Vimentin Enrichment in the Perinuclear Area. To further dissect the role of viral protein in vimentin rearrangement, we transfected vimentin-mCherry–expressing cells with EGFP-tagged Env protein and monitored vimentin dynamics. The results showed that during 1.5-h real-time monitoring after overnight transfection, vimentin filaments and viral Env protein accumulated next to the nucleus synchronously (Fig. 2*A* and Movie S3). By tracing the fluorescent intensity in the perinuclear region, vimentin was found to be gathered densely (Fig. 2*B*).

Moreover, the retrograde movement of vimentin filaments gather the scattered viral protein, as visualized by individual fluorescent foci, to the perinucleus region (Fig. 2*C* and Movie S4), indicating a potential role of vimentin being as a proviral factor. Considering a general phenomenon that vimentin could form a cage around aggregated protein during aggresome formation (34, 35), we performed a solubility assay to elaborate whether viral proteins might form aggregates to trigger vimentin rearrangement during ZIKV infection. The results showed that both viral Env and NS4B proteins gradually formed insoluble aggregates starting from 24 to 48 hpi (*SI Appendix*, Fig. S2*F*). However, the vimentin cage has already been formed at 16 to 24 hpi, which is apparent earlier than viral proteins forming aggregates (Fig. 1*A*). Consistent with the results in Fig. 1 *B–D*, these data suggest that vimentin in this context is not to be recruited by insoluble aggregates of viral proteins, but rather that viral protein production initiated from 16 hpi may serve as a trigger for vimentin rearrangement.

Host Vimentin Acts as an Organizer for the Integrity of Viral RCs and Is Required for Efficient Infection. Vimentin has gained more attention on its roles in various viral infections (16–21, 36). To determine whether there is a causal relationship between vimentin rearrangement and ZIKV infection, we used a CRISPR/Cas9 method to establish vimentin-knockout (KO) in U2OS and Huh7 cells, both of which are highly susceptible for ZIKV infection (12, 31) (*SI Appendix*, Fig. S3 *A* and *B*). Results showed that reducing vimentin levels neither affected the cell viability nor cell growth (*SI Appendix*, Fig. S3 *C–E*). We next used a lentiviral system to establish vimentin KO full-length rescue cells, and verified the levels of vimentin protein express in these cells by Western blot (*SI Appendix*, Fig. S3*A*).

In these cells, we observed not only similar vimentin network shrinkage and formation of a concrete compartment for viral RCs, but also viral protein localization at a subcellular level (Fig. 3*A*). Intriguingly, viral protein staining for NS4B, Env, and NS1 displayed a piecemeal and consistent distribution in vimentin KO cells (Fig. 3*A* and *SI Appendix*, Fig. S3 *F–H*), which is rarely seen in wild-type cells. It has been reported that the RCs during dengue virus type 2 (DENV-2) infection became diffused throughout the cytoplasm when vimentin was

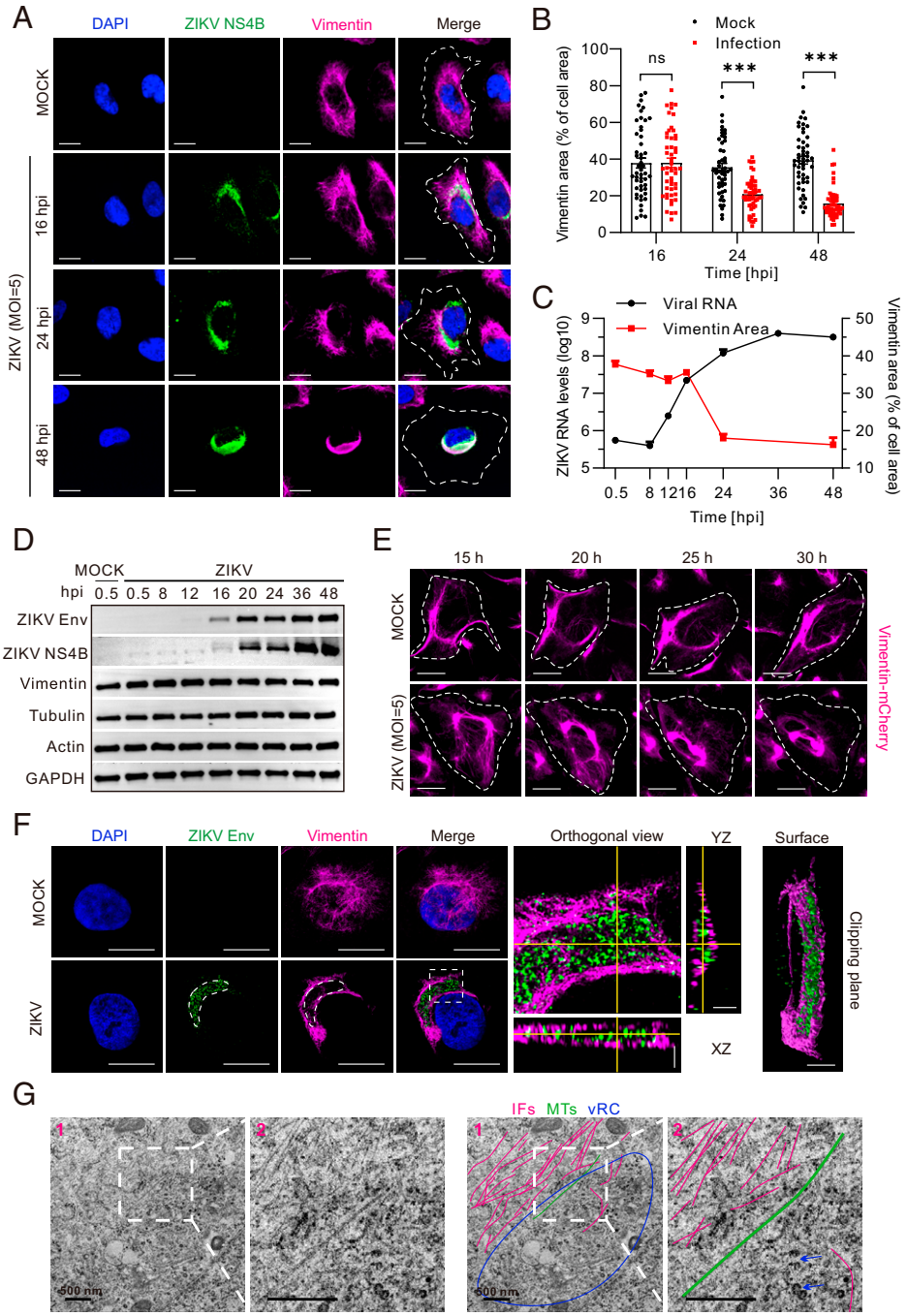

Fig. 1. Rearrangement of vimentin filaments in ZIKV-infected cells. (*A*) Human U2OS cells were infected with ZIKV (MOI = 5) for 16, 24, and 48 h. Viral NS4B protein and vimentin were stained with respective antibodies, and nucleus was stained with DAPI. The white dotted lines indicate the outline of the cells visualized by phalloidin-stained actin. (Scale bars, 15 μm.) (*B*) Quantification of the proportion of vimentin area versus overall cell area shown in *A*. Each point represents a single cell ($n = 50$) from three independent experiments. ***$P < 0.001$ (two-way ANOVA test). (*C*) Time course of the accumulated intracellular ZIKV RNA (MOI = 0.1) levels measured by qRT-PCR (corresponding to the left axis) and relative vimentin area changes (MOI = 5) (corresponding to the right axis), upon ZIKV infection. Error bars indicated means ± SEM from three independent experiments. (*D*) Time course of accumulated intracellular ZIKV Env and NS4B protein levels measured by Western blot in infected U2OS cells (MOI = 0.1). The expression levels of vimentin, tubulin, and actin were not affected by ZIKV infection with GAPDH as control. (*E*) The dynamic rearrangement of vimentin in vimentin-mCherry–expressing U2OS cells infected with ZIKV (MOI = 5). The white dotted lines indicate the outline of the cells. (Scale bars, 30 μm.) (*F*) Cells were immunostained for vimentin (magenta) and viral Env (green) at 24 hpi (MOI = 5), and visualized by 3D-SIM. White square (*Left*) indicates the magnified area shown in the corresponding color image (*Right*). Orthogonal sections and 3D reconstruction shows that vimentin encapsulates viral Env to form a cage-like structure. (Scale bars: 15 μm, *Left*; 2 μm, *Center* orthogonal view panel; 5 μm in the XZ panel; 5 μm in the YZ panel; and 5 μm in the *Right* clipping plane panel.) (*G*) Transmission electronic microscopy images of 70-nm-thin sections of resin-embedded cells infected with ZIKV (MOI = 5) for 24 h. White square indicates the magnified area shown in the corresponding color image on the *Right*. IFs, intermediate filaments indicated with magenta lines; MTs, microtubules indicated with green lines; vRCs, viral RCs indicated with blue circle. (Scale bars, 500 nm in the cell images and in the magnified images).

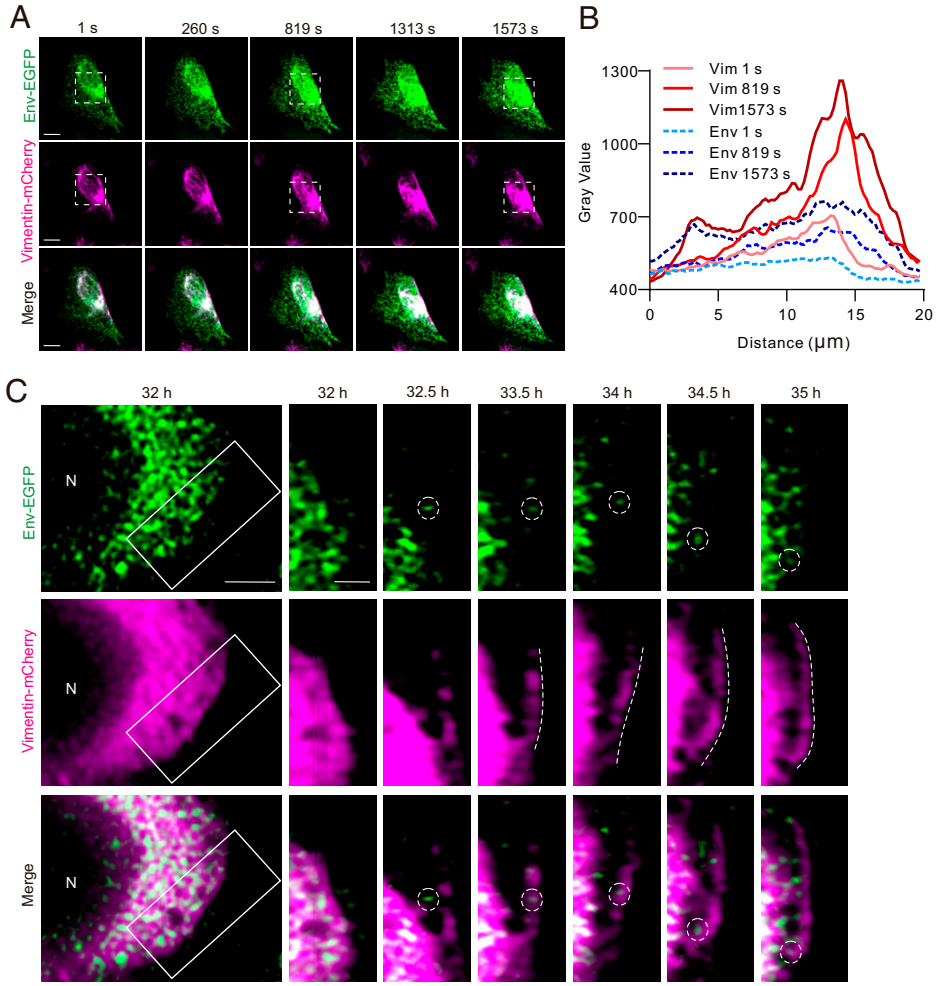

Fig. 2. Expression of ZIKV envelop protein induces vimentin rearrangement. (*A*) The dynamic rearrangement of vimentin in vimentin-mCherry–expressing U2OS cells transfected with ZIKV Env–EGFP plasmid (2 μg). (Scale bars, 10 μm.) (*B*) Plot profile analysis of Env–EGFP and vimentin-mCherry intensities in the white dotted box in *A* at corresponding time point. Distance in the *x* axis represents horizontal distance through the selection. (*C*) Vimentin filaments gather scattered viral Env protein toward peri-nucleus region. N and white box (*Left*) indicate cell nucleus and the magnified area shown in the corresponding *Right* panel. The dotted circles indicated the positions of one ZIKV-Env foci, and the dotted white lines indicated the shape of one vimentin filament. (Scale bars, 2 μm in the cell images and 1 μm in the magnified images.)

knocked down by small-interfering RNA (siRNA) (37). Differently, we witnessed here that ZIKV RCs are scattered into lumps rather than evenly diffused as in the DENV-2 case, indicating a distinct dispersion feature regulated by vimentin upon ZIKV infection. Moreover, depletion of vimentin dramatically increases the proportion of partitioned cellular viral protein compartments up to 85% and reduces the total viral protein area, both of which can be fully rescued when full-length vimentin was reintroduced (Fig. 3 *A*–*C*). Nevertheless, vimentin that forms unit-length filaments (ULF) or squiggles was not able to fully rescue the viral dispersion phenotype observed in infected cells (Fig. 3 *A* and *B*).

How does this scattered subcellular distribution of viral protein influence viral replication? To address this, we subsequently measured viral genome replication by qRT-PCR and viral protein expression by Western blot in vimentin KO cells. It is apparent that the absence of vimentin caused significant reduction of viral RNA copies and viral protein levels at both 24 and 48 hpi (Fig. 3 *D* and *E*), and reintroducing vimentin partially rescued the viral protein expression (Fig. 3*E*). Virus titer was further measured and, as expected, there was at least 20-fold less of viruses released from vimentin-depleted cells at 48 hpi (Fig. 3*F*). Similarly, in Huh7 cells, vimentin depletion showed defective infection as that in U2OS cells (*SI Appendix*, Fig. S3 *I*–*K*).

By immunostaining and flow cytometry, fewer infected cells were detected in a vimentin-depletion background at 24 and 48 hpi, the fast replication period during the viral life cycle (Fig. 3 *G* and *H*), suggesting that vimentin is critical for efficient ZIKV infection. Taken together, these data show that depletion of host vimentin leads to compromised viral infection, as demonstrated by less genome replication, reduced protein expression, and fewer particle production, most probably as a result of the disruption of the integrity of concentrated perinucleus RCs.

Vimentin Depletion Compromises Viral Genome and Protein Synthesis without Affecting Viral Binding and Entry to the Host Cell. To further investigate the function of vimentin, a time course of infection experiment was performed. Changes of viral RNA copies in wild-type and vimentin KO cells were confirmed by qRT-PCR. Although the viral RNA numbers were the same at the beginning of infection, their copies in vimentin KO cells were consistently lower than that in wild-type cells during the later period of infection (Fig. 4*A*). Apart from the replication dynamics of viral genome, viral proteins in both backgrounds accumulated gradually, but vimentin depletion led to a slower accumulation

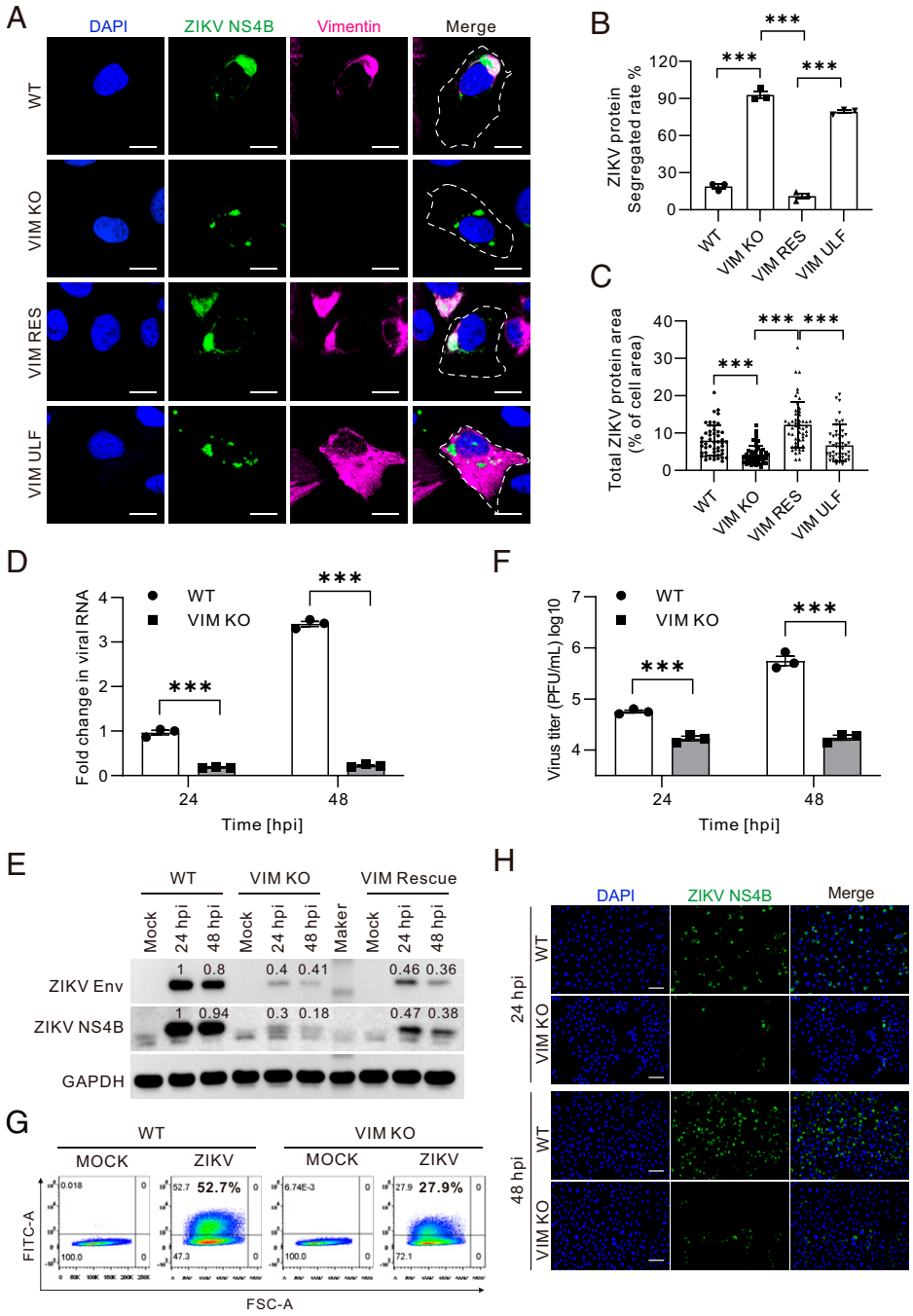

Fig. 3. Depletion of vimentin results in disruptive RCs and subsequent reduced ZIKV infection. (*A*) WT, vimentin KO (VIM KO), vimentin-full-length reintroducing (VIM RES), and vimentin ULF (VIM ULF) reintroducing cells were infected with ZIKV (MOI = 5) for 24 h. Cell were fixed and immunostained to visualize ZIKV NS4B, vimentin, and nucleus. (Scale bars, 15 μm.) (*B*) Quantification of the percentages of cells with segregated ZIKV Env in WT, VIM KO, VIM RES, and VIM ULF conditions. Results from three independent experiments and at least 10 fields of view each are shown. ***$P < 0.001$ (one-way ANOVA test). (*C*) Quantification of the percentage of total ZIKV protein area to overall cell area in WT, VIM KO, VIM RES, and VIM ULF conditions. Each point represents an infected cell ($n = 50$) from three independent experiments. ***$P < 0.001$ (one-way ANOVA test). (*D–F*) Intracellular ZIKV RNA (*D*), ZIKV Env and NS4B protein level (*E*), and titers of ZIKV particles (*F*) in infected WT and vimentin KO cells (MOI = 0.1) were measured by two-step qRT-PCR, Western blotting, and plaque assay, respectively. Numbers in the blots indicated the levels of ZIKV proteins normalized to GAPDH. Results from three independent experiments are shown. ***$P < 0.001$ (two-way ANOVA test). (*G*) Percentage of infected WT and VIM KO cells (MOI = 1, 48 hpi) measured by flow cytometry. (*H*) Percentage of infected WT and VIM KO cells (MOI = 5) measured by immunofluorescence. Cell were fixed and immunostained to visualize ZIKV NS4B and nucleus. (Scale bars, 100 μm.) Error bars indicated means ± SEM.

and, thus, much less viral Env and NS4B protein expression at each time point from 16 hpi onwards (e.g., 20, 24, 36, and 48 hpi), compared to wild-type cells (Fig. 4*B*).

The observed low levels of viral Env protein expression in vimentin KO cells could be due to a decrease in protein biogenesis and an increase in protein degradation. We therefore tested whether vimentin could influence the stability of ZIKV proteins. Plasmid expressing Env–EGFP and NS4B–EGFP fusion proteins were transiently transfected into cells, respectively, and analyzed by Western blot 48 h later (Fig. 4*C*).

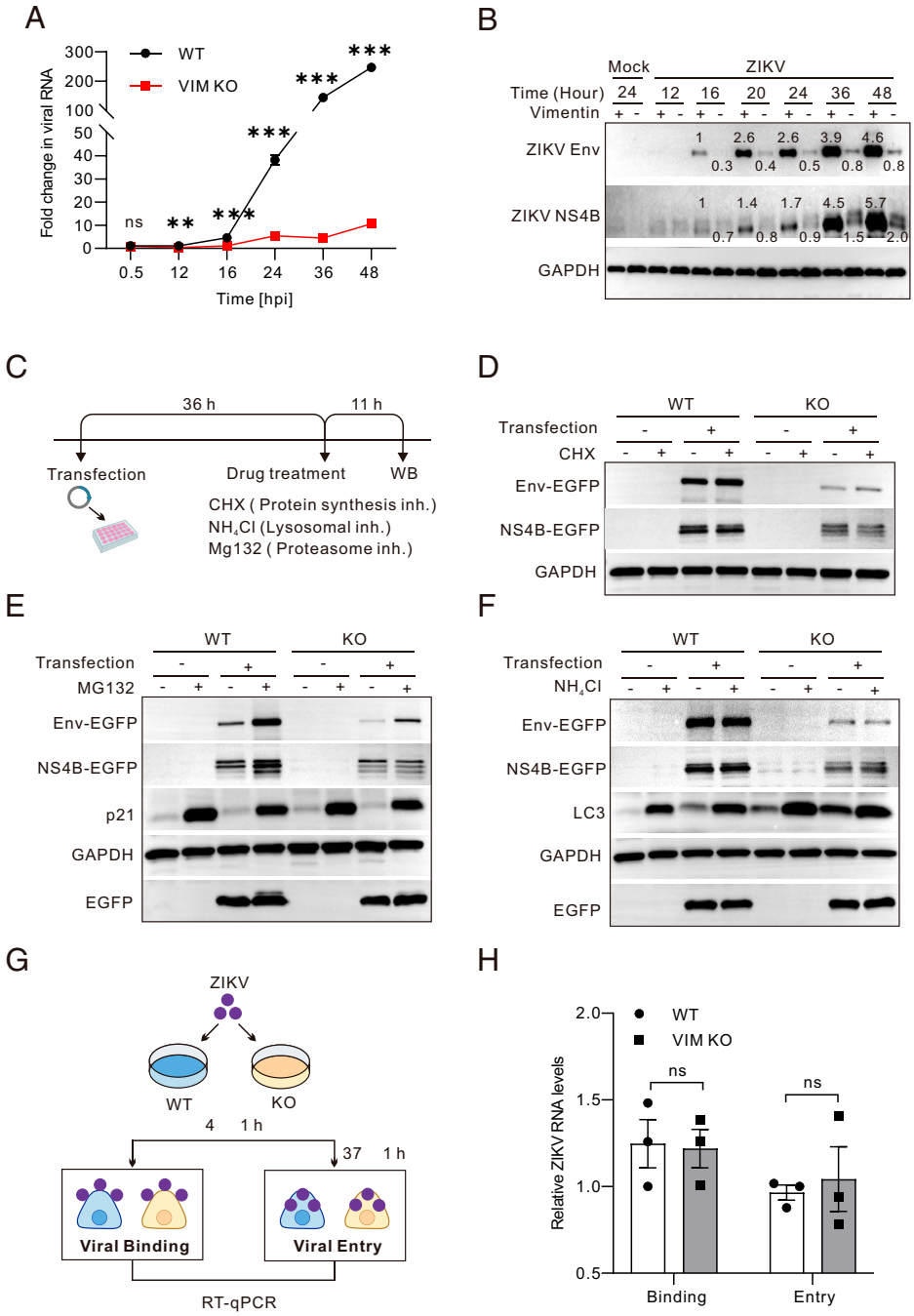

Fig. 4. Depletion of vimentin influences the production of viral components after entering cells. (*A*) Time course of accumulated intracellular ZIKV RNA in infected U2OS WT and VIM KO cells (MOI = 0.1) measured by qRT-PCR. The values were relative to WT at 0.5 hpi. Error bars indicated means ± SEM, ***$P < 0.001$ (unpaired *t* test). (*B*) Time course of accumulated intracellular ZIKV Env and NS4B protein in infected WT and VIM KO cells (MOI = 0.1) measured by Western blots. Numbers in the blots indicated the levels of ZIKV Env or NS4B normalized to GAPDH. (*C*) The schematic diagram of drug treatment experiment. Cells were transiently transfected with E-EGFP plasmid for 36 h, and then treated with MG132 (10 μM), NH_4Cl (25 mM), and CHX (20 μg/mL) for 11 h. (*D*) Western blotting analysis of viral protein upon CHX treatment. (*E*) Western blotting analysis of viral protein upon MG132 treatment, where detection of P21 accumulation serves as positive control. (*F*) Western blotting analysis of viral protein upon NH_4Cl treatment, where detection of LC3 accumulation serves as positive control. (*G*) The schematic diagram of ZIKV binding and entry assay. (*H*) ZIKV RNA levels from bound and internalized ZIKV were measured by qRT-PCR. Means ± SEM from three independent experiments is shown. ns $P > 0.05$ (two-way ANOVA test).

The results showed that vimentin depletion dramatically reduced the exogenous expression of both Env–EGFP and NS4B–EGFP (Fig. 4 *D–F*). We next treated cells with cycloheximide (CHX, 20 μg/mL for 11 h) to inhibit protein translation, and found that both viral Env and NS4B were relatively stable in both wild-type and vimentin KO cells (Fig. 4*D*). These suggest that vimentin acts on protein biosynthesis but not degradation. The following experiments further confirmed this assertion.

There are two classic destinations for cellular protein degradation regulated by proteasomal and lysosomal pathways. To further analyze whether depletion of vimentin promotes the degradation of viral protein and via which way, cells transfected with Env–EGFP and NS4B–EGFP, respectively, were treated

with proteasomal specific inhibitor MG132 (10 μM for 11 h), or lysosomal specific inhibitor ammonium chloride (NH_4Cl) (25 mM for 11 h) (Fig. 4*C*). Immunoblot analysis showed that the levels of Env and NS4B apparently increased after MG132 treatment (Fig. 4*E*), but were not influenced by NH_4Cl application (Fig. 4*F*). Concurrently, p21 and LC3, known proteins for proteasome and lysosomal degradation, respectively, were chosen as positive controls for these experiments. Combing results of the increased viral protein upon MG132 treatment but not NH_4Cl treatment, it is reasonable to conclude that viral proteins were degraded mainly via proteasomal pathway and vimentin depletion does not interrupt the degradation of viral protein.

Given that vimentin shrinking was visualized from 24 hpi but not before, we speculated that the early steps of viral replication were not affected in vimentin depletion cells. To confirm this, we used two assays to examine binding and entry steps (Fig. 4*H*), respectively. Cells were infected by ZIKV for 1 h at 4 °C, directly or incubated for 1 more hour at 37 °C, washed, and then cell lysates collected for measurement of RNA copies by qRT-PCR (Fig. 4*G*). The results confirmed that both the binding and entry of ZIKV are similarly efficient in wild-type and vimentin KO cells (Fig. 4*H*). Collectively, these results suggest that vimentin acts on the production and accumulation of ZIKV proteins as well as the efficient replication of ZIKV RNA, without influencing viral internalization.

A Large Number of Host RBPs Interact with and Are Being Regulated by Vimentin During ZIKV Infection. Since the perinuclear expression of vimentin is highly associated with the ER where viral RNA replication and protein translation take place, we speculate that aside from being a structural scaffold, vimentin may interact with host factors that regulate viral RNA transcription and subsequent protein synthesis. To test this, we implemented MS analysis to identify proteins interacting with vimentin, and subjected 1,050 candidates to gene ontology (GO) analyses by DAVID (The Database for Annotation, Visualization and Integrated Discovery). The recognized vimentin interactors were classified based on three taxonomic features, including molecular function, cellular component, and biological process. From the classification analysis, we found that a large proportion of candidates interacted with vimentin are RBPs and ribosome components (Fig. 5*A*), and they are intimately related to RNA processing, translation, and viral transcription (Fig. 5*B*). Importantly, GO annotation revealed a significant enrichment of ER components with vimentin (Fig. 5*C*), indicating that vimentin is the principal factor that interacts with ER-associated RBPs in host cells.

To complement with the interactome assay, RNA-seq was subsequently applied to analyze the variations of global gene transcription in both wild-type and vimentin KO cells infected with ZIKV. A total of 1,408 genes were significantly affected ($P < 0.05$), including 518 up- and 890 down-regulated genes in a vimentin-depletion background upon ZIKV infection (*SI Appendix*, Fig. S4*A*). Among the down-regulated hits, there are many ER-localized genes related to dsRNA binding and transcription regulation (*SI Appendix*, Fig. S4 *B* and *C*), as well as a large proportion of genes involved in antiviral immune and inflammatory response (Fig. 5*D*). Together with the MS result, we conclude that aside from contributing to RC scaffolding, which provides a structural support, vimentin is also involved in processing viral RNA replication and serving a functional role.

Given the critical role of ER in ZIKV infection, we more carefully examined candidates with ER localization in both MS and RNA-seq results (Fig. 5 *E* and *F*). By investigating ER-annotated candidates, we obtained the top 15 vimentin-interacting proteins by setting the threshold of interacting peptides coverage over 30% from MS results (Fig. 5*E* and *SI Appendix*, Table S1). Concurrently, RNA-seq data were analyzed and the results demonstrated dramatical changes of the mRNA levels of many ER-associated genes, among them, 80% of significantly differentially expressed genes were down-regulated (Fig. 5*F*). By cross-checking MS and RNA-seq candidates, ER-resident RRBP1 (also known as p180) was recognized as the only common hit, which shows high endogenous expression in wild-type and substantially down-regulated expression in vimentin KO cells during ZIKV infection (Fig. 5*F*). Of note, it has been recently reported that RRBP1 play a pronounced role in flaviviruses (e.g., DENV, ZIKV) infection by directly binding to viral RNA (38). We thus focused on RRBP1, and asked how the interaction between vimentin and RRBP1 influence ZIKV infection.

Host Vimentin Acts as a Regulator to Interact and Modulate ER-Resident RRBP1 to Facilitate ZIKV Infection. RRBP1 contains a short ER luminal domain, a transmembrane domain, and a large cytoplasmic domain containing a tandem repeat motif (39) (Fig. 6*A*). RRBP1 peptides interacting with vimentin identified from MS were located mostly in the cytoplasmic coiled-coil region (25 of 28 recognized peptides) (Fig. 6*A* and *SI Appendix*, Table S2). We subsequently performed the pull-down assay by using purified His-tagged vimentin protein with an RRBP1 antibody as probe. The results confirmed that RRBP1 indeed interacts with vimentin both in vitro and in cell-free conditions (Fig. 6*B*).

Next, we explored the correlation between the cellular expression of vimentin and RRBP1 upon ZIKV infection. Immunofluorescence results showed that in wild-type cells, both vimentin and RRBP1 are accumulated around the nucleus where the ER network resides (Fig. 6*C* and *SI Appendix*, Fig. S5 *G* and *H*). Upon ZIKV infection, both vimentin and RRBP1 aggregated near the nucleus and colocalized with dsRNA-staining positive viral RNA (Fig. 6*C* and *SI Appendix*, Fig. S5*A*), indicating both of them have participated in the viral RC process.

To elucidate the relationship between vimentin and RRBP1, we compared the RNA level, protein level, and the localization of RRBP1 in wild-type and vimentin KO cells. Results showed that depletion of vimentin reduced both the mRNA and protein levels of RRBP1 to around 50%, and enlarged the cellular distribution of RRBP1 (Fig. 6 *D* and *E* and *SI Appendix*, Fig. S5 *B–D*). In contrast, deprivation of RRBP1 neither affects the mRNA nor the protein level of vimentin (Fig. 6*G* and *SI Appendix*, Fig. S5*E*). Imaging data showed that lacking vimentin led to a decrease and concurrently expansion of the subcellular viral RNA and RRBP1 in infected cells (Fig. 6 *C–E* and *SI Appendix*, Fig. S5*F*).

Consistently, upon ZIKV infection, RRBP1 turned into scattered segregation in vimentin KO cells, similar as segregated viral proteins (Figs. 3*A* and 6*C*), indicating that disruption of RC integrity by vimentin influenced not only viral components but also host viral-binding components. It is subsequently noted that the colocalization between RRBP1 and viral dsRNA were significantly reduced, while the colocalization between RRBP1 and the ER was basically unchanged, in vimentin KO cells (Fig. 6 *C* and *F* and *SI Appendix*, Fig. S5 *H* and *J*), suggesting that vimentin depletion reduced the combined abundance of viral-host constituents in RCs, rather than the location of RRBP1 on the ER. Given the expansive distribution of ER-located RRBP1, we further investigated the effect of vimentin KO on ER morphology. Surprisingly, depletion of vimentin resulted in ER dispersion in both mock and ZIKV-infected conditions (*SI Appendix*, Fig. S5 *G–I*), suggesting that vimentin is critical for the subcellular distribution of the ER. Although dsRNA is colocated with the ER in both wild-type and vimentin KO cells (*SI Appendix*, Fig. S5 *G* and *H*), the ER tends to gather near the nucleus where viral dsRNA accumulates in wild-type cells, and becomes piecemeal together with dsRNA in vimentin KO

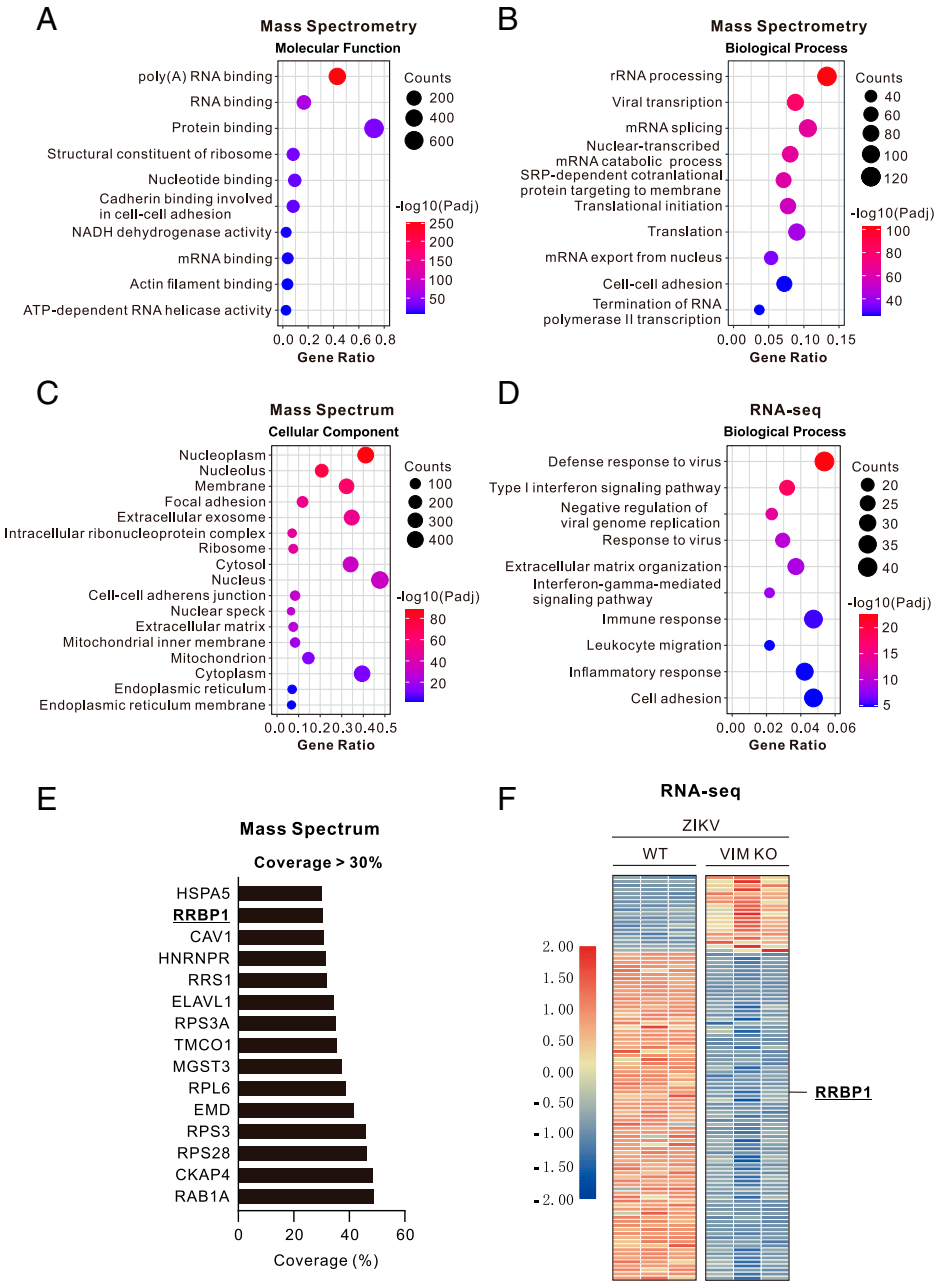

Fig. 5. Interaction between vimentin and ER-localized RNA-binding components affect ZIKV infection. (*A–C*) GO analysis of proteins interacting with vimentin in A549 cells. (*A*) The top 10 significant GO terms in molecular function are shown in the bubble chart. (*B*) The top 10 significant GO terms in biological process are shown in the bubble chart. (*C*) All 17 significant cellular components with count number greater than 50 genes are shown in the bubble chart. (*D*) Biological process enrichment analysis of significantly down-regulated genes in ZIKV-infected VIM KO cells compared with infected WT cells (MOI = 1, 24 hpi) by RNA-seq. The top 10 enriched terms are shown in the bubble chart. In *A–D*, the color of the bubbles displayed from red to blue indicated the descending order of -log10(P_{adj}). The sizes of the bubbles are displayed from small to large in ascending order of gene counts. The *x* and *y* axis represent the gene ratio and the GO terms, respectively. (*E*) List of ER-located proteins interacting with vimentin by setting the coverage peptides threshold over 30% from MS assay. (*F*) Heatmap of significantly differentially expressed genes (ER-annotated) between ZIKV infected U2OS WT and VIM KO cells (MOI = 1, 24 hpi) identified by RNA-seq (n = 3 independent experiments per condition).

cells (*SI Appendix*, Fig. S5 *G–J*), indicating that remodeled ER subcellular localization is the reason for the scattered distribution of viral RC. Together, these data suggest that the intimate connection between vimentin and the ER is essential for elaborate remodeling of the ER during latter stages of ZIKV infection, ensuring the viral RC concentration around the nucleus.

The above results suggested that ER-located RRBP1 assists viral RNA replication by close contact with viral RNA, and this contact is regulated by vimentin. To verify this, we generated RRBP1 knockdown (KD) cells in both wild-type and vimentin KO background by short-hairpin RNA (shRNA) (Fig. 6*G* and *SI Appendix*, Fig. S5 *D* and *E*) and then infected them with ZIKV. Consistent with a previous study (38), RRBP1 KD reduced viral RNA copies by about 40% (Fig. 6*H*). In comparison, the effect of vimentin depletion on the reduction of viral genome replication was much more severe than that of RRBP1 KD; however, the double depletion has no additive effects (Fig. 6*H*), suggesting that RRBP1 and vimentin located in the same

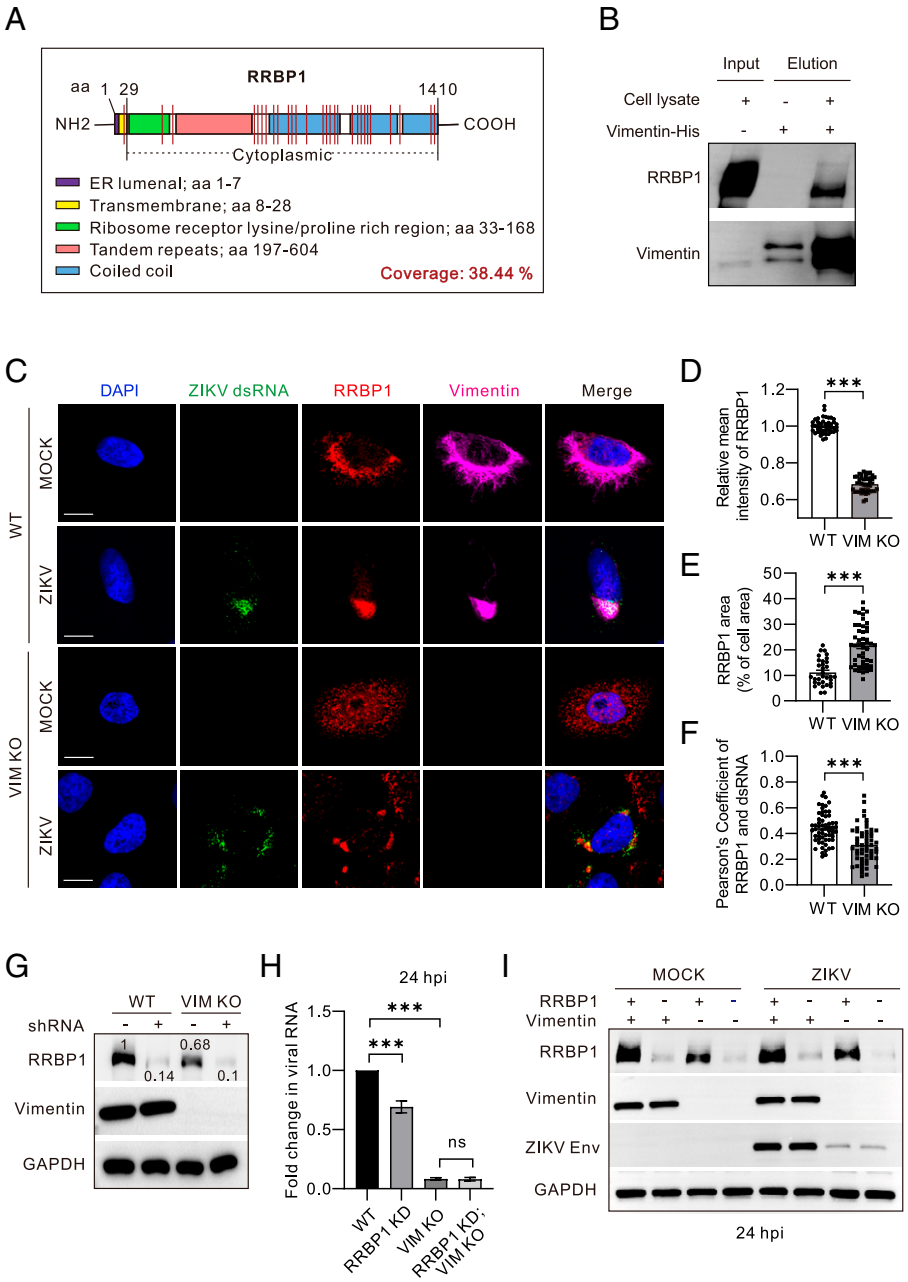

Fig. 6. Vimentin interacts with ER-located RRBP1 to regulate ZIKV infection. (*A*) The domain structure of RRBP1 protein. Red lines represent the peptides interacting with vimentin identified from MS. (*B*) In vitro binding assay of vimentin with RRBP1. Cell lysates were incubated with purified recombinant his-tagged vimentin protein, and analyzed by anti-RRBP1 antibody in Western blotting. (*C*) Immunofluorescence images of vimentin, RRBP1, and ZIKV RNA in WT and VIM KO cells infected with ZIKV (MOI = 5) for 24 h, and stained with anti-dsRNA, anti-RRBP1, and antivimentin antibodies and DAPI for nucleus. (Scale bars, 15 μm.) (*D* and *E*) Quantifications of RRBP1 intensities (*D*) and areas (*E*) in noninfected (MOCK) WT and VIM KO cells. Each point represents a single cell. ***$P < 0.001$ (unpaired *t* test). (*F*) Quantification of the colocalization between RRBP1 and dsRNA in ZIKV-infected WT and VIM KO cells by Pearson's coefficients. Each point represents a single cell. ***$P < 0.001$ (unpaired *t* test). (*G*) Western blots demonstrated that RRBP1 was efficiently knocked down by shRNA in both WT and VIM KO cells. Numbers in the blots indicated the levels of RRBP1 normalized to GAPDH. (*H*) Quantifications of ZIKV RNA copies detected by qRT-PCR, and normalized to GAPDH, in WT, RRBP1 KD, VIM KO, and RRBP1 KD;VIM KO conditions. The cells were infected with ZIKV at MOI = 0.1 for 24 h, and the data are from three independent experiments. ***$P < 0.001$ (one-way ANOVA test). (*I*) Protein levels of RRBP1, vimentin, ZIKV Env in WT and vimentin KO cells detected by Western blots, which were also probed with vimentin antibody to confirm the KO efficiency and GAPDH antibody to verify equal sample loading.

regulating cascade during ZIKV infection. Next, synthesized viral protein was analyzed. The absence of vimentin resulted in significant reduction of structural protein Env, but the absence of RRBP1 alone showed no obvious effect (Fig. 6*I*), indicating that RRBP1 plays a role in viral RNA replication rather than protein synthesis. Taken together, these results demonstrate a pivotal role of vimentin as an upstream factor regulating one of the known viral-binding host factors, RRBP1, to affect viral RNA replication. Combined with omics analysis, these data further suggest that aside from contributing to scaffolding RCs, vimentin also acts as a hub molecule to interact with and regulate various RBPs. Both functions of vimentin are important

for facilitating efficient ZIKV replication and promoting infection.

Discussion

In this study, we report the spatial-temporal rearrangement of vimentin filaments induced by ZIKV infection. Importantly, we reveal two major functions of host cell vimentin during ZIKV infection: 1) organizer, as a structural support to increase the local concentration of all necessary factors for high efficiency of viral replication; and 2) regulator, by interacting with and regulating RBPs, such as RRBP1, to facilitate viral replication. The latter is unique as a time that vimentin has been demonstrated to play a nonscaffold function in the context of virus infection. Moreover, as vimentin provides a structural cage surrounding RCs as organizer, their concentration also increases near RCs that can positively enhance its regulator role. These two roles complement one another to make an integrated view of vimentin in regulating ZIKV replication.

Vimentin Cage Formation in Viral Infections. Viral infections rewire cellular networks, especially endomembrane and cytoskeleton, to generate the viral RCs for efficient replication (11). Thereby, various virus-induced structures—such as convoluted membrane, zippered ER, invaginated vesicles, and vesicle packet—play a crucial role in viral morphogenesis (13, 40, 41). However, the spatial structure features and the mechanisms of morphological maintenance of such a complex remain elusive. Our present study uses ZIKV to examine this issue. ZIKV infection induces nestin, one of the IFs in neural stem and progenitor cells, to restructure in the perinuclear region to wrap around viral dsRNA (12). Although it has been reported that ZIKV dsRNA colocalized with vimentin filaments to the perinuclear region (42), the dynamic spatial correlation between vimentin filaments and viral proteins of ZIKV, as well as the function of vimentin in ZIKV infection, are unknown. Taking advantage of imaging techniques, we found that ZIKV infection led to vimentin remodeling and formation of cage-like structures that surround the RCs, long after the initiation of viral RNA replication, but following more closely to viral protein production (Fig. 1 *C* and *E*). This kinetic association between host vimentin and viral products has been demonstrated by several lines of evidence. 1) The appearance of vimentin shrinking was ~16 h from the commencement of infection, coincides with the period of exponential increase of viral RNA replication (Fig. 1*C*). 2) Vimentin filaments gradually accumulated to the site of viral protein synthesis or RCs, to eventually form a whole cage (Fig. 1*A*). 3) The cages could also be formed when cells started to synthesis new viral proteins (Fig. 2 *A* and *C*). Finally, 4) cage formation was not observed in cases where only EGFP vectors were expressed, or medium without live viruses was included (*SI Appendix*, Fig. S1*G*). Despite being unable to prove a cause-and-effect mechanism yet, the above data strongly suggest a link between ZIKV infection and vimentin function.

In agreement with our data, vimentin rearrangement has been observed in other experimental models of infection. In cells with DENV-2 infection, vimentin has increased the interaction with viral NS4A protein, and vimentin filaments gradually moved toward the nucleus, and finally formed cage structures at around 48 hpi (37). In SARS-CoV-2 infection, the beginning of vimentin retraction falls within the time frame (around 6.5 hpi) of genome replication (43). We first characterize the spatial-temporal characteristics of vimentin filaments in ZIKV infection. Both the time of appearance and the colocalization in the perinuclear area for the replication-assembly organelles, lead us to interpret that vimentin sensed viral replication and formed a scaffold to facilitate viral replication.

The Need of Vimentin in Viral Infections. In line with the hypothesis that the cytoskeleton cage observed in ZIKV infection might contribute to spatially concentration of different viral-induced membranous structures (12), we demonstrated that without the cage formation after vimentin depletion, the ER is more dispersive (*SI Appendix*, Fig. S5 *G–I*), and RCs are misorganized and segregated in the cytoplasm (Fig. 3*A*), leading to less efficient synthesis of viral components, and lower overall infection efficiency (Figs. 3 *A*, *D–H* and 4 *A* and *B*). Several studies report IFs link to membranous organelles, such as mitochondria (44), Golgi (45), and lysosome (46, 47). The relationship between vimentin and the ER, especially in infection conditions, is worthy of future study. Moreover, disruption of vimentin filaments by a chemical Acrylamide significantly reduced the release of both bluetongue virus and DENV-2 (48, 49). Treatment with Withaferin A, a compound that disrupts vimentin network, resulted in a significant reduction in SARS-CoV-2 replication and virion released (43). Thus, it may be a common function in viral infection that vimentin cage organizes the replication structures and provides an optimal niche for the replication/translation to occur.

The decreased viral protein level within cells may be due to the reduced production or increased degradation. Vimentin has been previously shown to regulate the proteasomal degradation of hepatitis C virus (HCV) core protein to affect HCV production (50). In contrast, by treatment with protein synthesis and degradation inhibitors, we showed that ZIKV Env biogenesis, but not its stability, was reduced in vimentin-depleted cells (Fig. 4 *C–F*). Thus, why vimentin acts differently in different viral infections remains to be determined.

The Nonstructural Role of Vimentin in Viral Infections. The ER is an essential cellular compartment for completion of the virus life cycle. During ZIKV replication, there is an accumulation of viral components in the ER (13), and viral nonstructural proteins can be incorporated into the ER membrane to create invagination or protrusion vesicles for viral RNA replication (11).

Since viruses cannot encode all proteins necessary for their life cycle, they usurp cellular protein biogenesis machineries, such as ribosomal proteins (51), RBPs for viral RNA replication/transcription (52–54), and formation of the ER membrane protein complex (55, 56). Noncoding subgenomic flavivirus RNA (sfRNA) produced by ZIKV can interact with over 20 RBPs to regulate multiple cellular posttranscriptional processes, and therefore limit effective response of these cells to viral infection (57, 58). Four-hundred and sixty-four RBPs were identified as being associated with DENV or ZIKV guide RNAs, including previously reported candidates (e.g., heterogeneous nuclear ribonucleoproteins, polyadenylate-binding protein) that specifically associate with DENV RNA (38, 59–61), and recently known RBPs vigilin and RRBP1, which were reported to directly bind to DENV and ZIKV RNA (38).

In line with these discoveries, using MS and RNA-seq analysis, we revealed that vimentin interacts with a large number of RBPs and ribosomal proteins to regulate cellular transcription and translation, enabling efficient ZIKV replication (Fig. 5). Importantly, numbers of ER-located proteins interacting with vimentin revealed from our screen data have been previously demonstrated in ZIKV infection. For example, the chaperone activity of binding immunoglobulin protein (BiP/GRP78/HSPA5) promotes ZIKV infection by interacting with viral envelop protein and cellular alkaline phosphatase (62–66). ELAV-like RNA binding protein 1 (ELAVL1/HuR) interacts with HCV 3′UTR and increased HCV replication (67), whereas it exhibits an antiviral effect in ZIKV infection (68). KD of HYOU1 have dramatically reduced the viral titer of both ZIKV and DENV (64). It is intriguing that our RNA-seq results

reveal depletion of vimentin significantly reduced HYOU1 level (Fig. 5*F*). Considering the interplay between cytoskeleton and the ER membrane (69–72), it is tempting to speculate that virus-induced vimentin cage not only provides physical space for viral RCs accumulation, but equally importantly, interacts with molecules involved in cellular transcription and translation process, and thus promotes the efficiency of virus replication from perspectives of both physical support and functional control.

The Interaction between Vimentin and RRBP1. Among the numerous candidates, we focused on the interaction between vimentin and RRBP1, a positively charged membrane-bound protein found in rough ER (73), because: 1) RRBP1 was identified as the top candidates in both MS and RNA-seq examinations; and 2) RRBP1 could directly bind viral RNA and play a pronounced role during DENV and ZIKV infection (38).

A previous study has identified that RRBP1 could mediate the interaction between the ER and MTs via the novel MT-binding and -bundling domain MTB-1 of the coiled-coil region of RRBP1 (27). Overexpression of MTB-1 induced acetylated MTs and promoted MT bundling (27). Moreover, RRBP1 also regulates ER organization and controls axon specification by regulating local MT remodeling (28). Aside from the interplay with MTs, our data demonstrate that RRBP1 colocalizes with ZIKV dsRNA, and KD of RRBP1 in wild-type cells reduces ZIKV RNA replication (Fig. 6 *C* and *H*).

Significantly, our results are unique in identifying that vimentin can directly bind to RRBP1 and influence its cellular localization and expression level in both mock-infected and ZIKV-infected cells. Since vimentin is generally considered to play mechanical roles, such as improving the mechanical integrity of cells and determining the mechanical strength and resilience of cells in recent years (74), our discovery represents an improved understanding of the regulator role of vimentin, and the interplay between cytoskeletal IFs and ER proteins, especially in the context of virus infection. Of note, RRBP1 depletion has less effect on viral replication than that of vimentin depletion (Fig. 6 *H* and *I*), and RRBP1 expression has no significant influence on the cellular distribution, mRNA and protein expression of vimentin, indicating RRBP1 acts through vimentin during ZIKV infection. Further investigation is needed to determine whether other RBPs may cooperate with vimentin to modulate ZIKV replication, and whether this cooperation is a universal phenomenon during flavivirus infection. Identification of these factors not only benefits the characterization of the biogenesis of ZIKV RCs, but also provides potential candidates for developing broad-spectrum compounds that restrict viral replication.

Materials and Methods

Human U2OS cells and Huh7 cells (and derived KO and full-length rescue cells) were infected with ZIKV (SZ01 strain). Infected cells were analyzed for RNA replication, protein expression, infectious virus production, viral RC localization, and GO by qRT-PCR, Western blot, plague, immunofluorescence, transmission electron microscopy, MS, and RNA-seq. The detailed information of these techniques is described in *SI Appendix*.

Data Availability. The MS proteomics data have been deposited to the ProteomeXchange Consortium via the publicly accessible PRIDE partner repository (dataset identifier PXD027362). All RNA-seq data have been deposited into the publicly accessible CNGB Sequence Archive (CNSA) of China National GeneBank DataBase (CNGBdb) (accession no. CNP0002016). All other study data are included in the main text and *SI Appendix*.

ACKNOWLEDGMENTS. We thank John E. Eriksson (University of Turku and Åbo Akademi University, Finland) for providing us the vimentin plasmids; and Lan Bao (Chinese Academy of Science), Pekka Lappalainen (University of Helsinki, Finland), and Xueliang Zhu (Chinese Academy of Science) for insightful discussion. This study was supported by Key Research and Development Program, Ministry of Science and Technology of China (2021YFC2300204); the National Natural Science Foundation of China (92054104, 31970660); the Chinese Academy of Science-Vice Presidency Science and Technology Silk Road Science Fund (GJHZ2021138); the Shanghai Municipal Science and Technology Major Project (2019SHZDZX02); the Key Laboratory of Molecular Virology & Immunology, Institut Pasteur of Shanghai (KLMVI-OP-202001); and the Strategic Priority Research Program of the Chinese Academy of Sciences (XDA13010500).

1. V. M. Cao-Lormeau *et al.*, Guillain-Barré Syndrome outbreak associated with Zika virus infection in French Polynesia: A case-control study. *Lancet* **387**, 1531–1539 (2016).
2. T. C. Pierson, B. S. Graham, Zika virus: Immunity and vaccine development. *Cell* **167**, 625–631 (2016).
3. S. A. Rasmussen, D. J. Jamieson, M. A. Honein, L. R. Petersen, Zika virus and birth defects—Reviewing the evidence for causality. *N. Engl. J. Med.* **374**, 1981–1987 (2016).
4. T. C. Pierson, M. S. Diamond, The emergence of Zika virus and its new clinical syndromes. *Nature* **560**, 573–581 (2018).
5. G. A. Poland, I. G. Ovsyannikova, R. B. Kennedy, Zika vaccine development: Current status. *Mayo Clin. Proc.* **94**, 2572–2586 (2019).
6. D. Musso, D. J. Gubler, Zika virus. *Clin. Microbiol. Rev.* **29**, 487–524 (2016).
7. A. Munjal *et al.*, Advances in developing therapies to combat Zika virus: Current knowledge and future perspectives. *Front. Microbiol.* **8**, 1469 (2017).
8. I. Lee *et al.*, Probing molecular insights into Zika virus–host interactions. *Viruses* **10**, 233 (2018).
9. Y. Shi, G. F. Gao, Structural biology of the Zika virus. *Trends Biochem. Sci.* **42**, 443–456 (2017).
10. D. Sirohi, R. J. Kuhn, Zika virus structure, maturation, and receptors. *J. Infect. Dis.* **216** (suppl. 10), S935–S944 (2017).
11. C. J. Neufeldt, M. Cortese, E. G. Acosta, R. Bartenschlager, Rewiring cellular networks by members of the Flaviviridae family. *Nat. Rev. Microbiol.* **16**, 125–142 (2018).
12. M. Cortese *et al.*, Ultrastructural characterization of Zika virus replication factories. *Cell Rep.* **18**, 2113–2123 (2017).
13. M. I. Mohd Ropidi, A. S. Khazali, N. Nor Rashid, R. Yusof, Endoplasmic reticulum: A focal point of Zika virus infection. *J. Biomed. Sci.* **27**, 27 (2020).
14. J. Lowery, E. R. Kuczmarski, H. Herrmann, R. D. Goldman, Intermediate filaments play a pivotal role in regulating cell architecture and function. *J. Biol. Chem.* **290**, 17145–17153 (2015).
15. F. Danielsson, M. K. Peterson, H. Caldeira Araújo, F. Lautenschläger, A. K. B. Gad, Vimentin diversity in health and disease. *Cells* **7**, 147 (2018).
16. K. Döhner, B. Sodeik, The role of the cytoskeleton during viral infection. *Curr. Top. Microbiol. Immunol.* **285**, 67–108 (2005).
17. K. Y. Foo, H. Y. Chee, Interaction between flavivirus and cytoskeleton during virus replication. *BioMed Res. Int.* **2015**, 427814 (2015).
18. C. E. Denes, M. Miranda-Saksena, A. L. Cunningham, R. J. Diefenbach, Cytoskeletons in the closet-subversion in alphaherpesvirus infections. *Viruses* **10**, 79 (2018).
19. Y. Zhang, W. Gao, J. Li, W. Wu, Y. Jiu, The role of host cytoskeleton in flavivirus infection. *Virol. Sin.* **34**, 30–41 (2019).
20. I. Ramos, K. Stamatakis, C. L. Oeste, D. Pérez-Sala, Vimentin as a multifaceted player and potential therapeutic target in viral infections. *Int. J. Mol. Sci.* **21**, 4675 (2020).
21. Y. Zhang *et al.*, The diverse roles and dynamic rearrangement of vimentin during viral infection. *J. Cell Sci.* **134**, jcs250597 (2020).
22. S. Kim, P. A. Coulombe, Emerging role for the cytoskeleton as an organizer and regulator of translation. *Nat. Rev. Mol. Cell Biol.* **11**, 75–81 (2010).
23. D. Hamill, J. Davis, J. Drawbridge, K. A. Suprenant, Polyribosome targeting to microtubules: Enrichment of specific mRNAs in a reconstituted microtubule preparation from sea urchin embryos. *J. Cell Biol.* **127**, 973–984 (1994).
24. O. Medalia *et al.*, Macromolecular architecture in eukaryotic cells visualized by cryoelectron tomography. *Science* **298**, 1209–1213 (2002).
25. J. Sotelo-Silveira, M. Crispino, A. Puppo, J. R. Sotelo, E. Koenig, Myelinated axons contain beta-actin mRNA and ZBP-1 in periaxoplasmic ribosomal plaques and depend on cyclic AMP and F-actin integrity for in vitro translation. *J. Neurochem.* **104**, 545–557 (2008).
26. S. Kim, J. Kellner, C. H. Lee, P. A. Coulombe, Interaction between the keratin cytoskeleton and eEF1Bgamma affects protein synthesis in epithelial cells. *Nat. Struct. Mol. Biol.* **14**, 982–983 (2007).
27. K. Ogawa-Goto *et al.*, p180 is involved in the interaction between the endoplasmic reticulum and microtubules through a novel microtubule-binding and bundling domain. *Mol. Biol. Cell* **18**, 3741–3751 (2007).
28. G. G. Farías *et al.*, Feedback-driven mechanisms between microtubules and the endoplasmic reticulum instruct neuronal polarity. *Neuron* **102**, 184–201.e8 (2019).
29. Y. Jiu *et al.*, Bidirectional interplay between vimentin intermediate filaments and contractile actin stress fibers. *Cell Rep.* **11**, 1511–1518 (2015).
30. K. Rausch *et al.*, Screening bioactives reveals nanchangmycin as a broad spectrum antiviral active against Zika virus. *Cell Rep.* **18**, 804–815 (2017).
31. B. A. Hackett *et al.*, Sirtuin inhibitors are broadly antiviral against arboviruses. *MBio* **10**, e01446-19 (2019).

32. S. Welsch *et al.*, Composition and three-dimensional architecture of the dengue virus replication and assembly sites. *Cell Host Microbe* **5**, 365–375 (2009).
33. L. A. Caldas, R. C. Azevedo, J. L. da Silva, W. de Souza, Microscopy analysis of Zika virus morphogenesis in mammalian cells. *Sci. Rep.* **10**, 8370 (2020).
34. J. A. Johnston, C. L. Ward, R. R. Kopito, Aggresomes: A cellular response to misfolded proteins. *J. Cell Biol.* **143**, 1883–1898 (1998).
35. R. García-Mata, Z. Bebök, E. J. Sorscher, E. S. Sztul, Characterization and dynamics of aggresome formation by a cytosolic GFP-chimera. *J. Cell Biol.* **146**, 1239–1254 (1999).
36. Z. Wen, Y. Zhang, Z. Lin, K. Shi, Y. Jiu, Cytoskeleton—A crucial key in host cell for coronavirus infection. *J. Mol. Cell Biol.* **12**, 968–979 (2020).
37. C. S. Teo, J. J. Chu, Cellular vimentin regulates construction of dengue virus replication complexes through interaction with NS4A protein. *J. Virol.* **88**, 1897–1913 (2014).
38. Y. S. Ooi *et al.*, An RNA-centric dissection of host complexes controlling flavivirus infection. *Nat. Microbiol.* **4**, 2369–2382 (2019).
39. D. W. Reid, C. V. Nicchitta, Diversity and selectivity in mRNA translation on the endoplasmic reticulum. *Nat. Rev. Mol. Cell Biol.* **16**, 221–231 (2015).
40. S. Miller, J. Krijnse-Locker, Modification of intracellular membrane structures for virus replication. *Nat. Rev. Microbiol.* **6**, 363–374 (2008).
41. A. Shulla, G. Randall, (+) RNA virus replication compartments: A safe home for (most) viral replication. *Curr. Opin. Microbiol.* **32**, 82–88 (2016).
42. I. Pagani *et al.*, Human endometrial stromal cells are highly permissive to productive infection by Zika virus. *Sci. Rep.* **7**, 44286 (2017).
43. M. Cortese *et al.*, Integrative imaging reveals SARS-CoV-2-induced reshaping of subcellular morphologies. *Cell Host Microbe* **28**, 853–866.e5 (2020).
44. O. E. Nekrasova *et al.*, Vimentin intermediate filaments modulate the motility of mitochondria. *Mol. Biol. Cell* **22**, 2282–2289 (2011).
45. Y. Gao, E. Sztul, A novel interaction of the Golgi complex with the vimentin intermediate filament cytoskeleton. *J. Cell Biol.* **152**, 877–894 (2001).
46. M. L. Styers *et al.*, The endo-lysosomal sorting machinery interacts with the intermediate filament cytoskeleton. *Mol. Biol. Cell* **15**, 5369–5382 (2004).
47. O. Biskou *et al.*, The type III intermediate filament vimentin regulates organelle distribution and modulates autophagy. *PLoS One* **14**, e0209665 (2019).
48. B. Bhattacharya, R. J. Noad, P. Roy, Interaction between Bluetongue virus outer capsid protein VP2 and vimentin is necessary for virus egress. *Virol. J.* **4**, 7 (2007).
49. R. Kanlaya, S. N. Pattanakitsakul, S. Sinchaikul, S. T. Chen, V. Thongboonkerd, Vimentin interacts with heterogeneous nuclear ribonucleoproteins and dengue nonstructural protein 1 and is important for viral replication and release. *Mol. Biosyst.* **6**, 795–806 (2010).
50. Y. Nitahara-Kasahara *et al.*, Cellular vimentin content regulates the protein level of hepatitis C virus core protein and the hepatitis C virus production in cultured cells. *Virology* **383**, 319–327 (2009).
51. R. K. Campos *et al.*, RPLP1 and RPLP2 are essential flavivirus host factors that promote early viral protein accumulation. *J. Virol.* **91**, e01706-16 (2017).
52. M. Garcia-Moreno, A. I. Järvelin, A. Castello, Unconventional RNA-binding proteins step into the virus-host battlefront. *Wiley Interdiscip. Rev. RNA* **9**, e1498 (2018).
53. K. Dicker, A. I. Jarvelin, M. Garcia-Moreno, A. Castello, The importance of virion-incorporated cellular RNA-Binding Proteins in viral particle assembly and infectivity. *Semin. Cell Dev. Biol.* **111**, 108–118 (2021).
54. M. Diosa-Toro, K. R. Prasanth, S. S. Bradrick, M. A. Garcia Blanco, Role of RNA-binding proteins during the late stages of flavivirus replication cycle. *Virol. J.* **17**, 60 (2020).
55. N. J. Barrows *et al.*, Dual roles for the ER membrane protein complex in flavivirus infection: Viral entry and protein biogenesis. *Sci. Rep.* **9**, 9711 (2019).
56. D. L. Lin *et al.*, The ER membrane protein complex promotes biogenesis of dengue and Zika virus non-structural multi-pass transmembrane proteins to support infection. *Cell Rep.* **27**, 1666–1674.e4 (2019).
57. D. Michalski *et al.*, Zika virus noncoding sfRNAs sequester multiple host-derived RNA-binding proteins and modulate mRNA decay and splicing during infection. *J. Biol. Chem.* **294**, 16282–16296 (2019).
58. S. Jansen *et al.*, Identification of host factors binding to dengue and Zika virus subgenomic RNA by efficient yeast three-hybrid screens of the human ORFeome. *RNA Biol.* **18**, 732–744 (2021).
59. S. L. Phillips, E. J. Soderblom, S. S. Bradrick, M. A. Garcia-Blanco, Identification of proteins bound to dengue viral RNA in vivo reveals new host proteins important for virus replication. *MBio* **7**, e01865-15 (2016).
60. O. V. Viktorovskaya, T. M. Greco, I. M. Cristea, S. R. Thompson, Identification of RNA binding proteins associated with dengue virus RNA in infected cells reveals temporally distinct host factor requirements. *PLoS Negl. Trop. Dis.* **10**, e0004921 (2016).
61. P. Scaturro, A. L. Kastner, A. Pichlmair, Chasing intracellular Zika virus using proteomics. *Viruses* **11**, 878 (2019).
62. J. Chen *et al.*, Placental alkaline phosphatase promotes Zika virus replication by stabilizing viral proteins through BIP. *MBio* **11**, e01716-20 (2020).
63. J. Royle *et al.*, Glucose-regulated protein 78 interacts with Zika virus envelope protein and contributes to a productive infection. *Viruses* **12**, 524 (2020).
64. R. Aviner, K. H. Li, J. Frydman, R. Andino, Cotranslational prolyl hydroxylation is essential for flavivirus biogenesis. *Nature* **596**, 558–564 (2021).
65. A. A. Elfiky, I. M. Ibrahim, Zika virus envelope–heat shock protein A5 (GRP78) binding site prediction. *J. Biomol. Struct. Dyn.* **39**, 5248–5260 (2021).
66. S. Khongwichit *et al.*, A functional interaction between GRP78 and Zika virus E protein. *Sci. Rep.* **11**, 393 (2021).
67. S. Shwetha *et al.*, HuR displaces polypyrimidine tract binding protein to facilitate La binding to the 3′ untranslated region and enhances hepatitis C virus replication. *J. Virol.* **89**, 11356–11371 (2015).
68. G. Bonenfant *et al.*, Zika virus subverts stress granules to promote and restrict viral gene expression. *J. Virol.* **93**, e00520-19 (2019).
69. M. Terasaki, L. B. Chen, K. Fujiwara, Microtubules and the endoplasmic reticulum are highly interdependent structures. *J. Cell Biol.* **103**, 1557–1568 (1986).
70. C. Risco *et al.*, Endoplasmic reticulum-Golgi intermediate compartment membranes and vimentin filaments participate in vaccinia virus assembly. *J. Virol.* **76**, 1839–1855 (2002).
71. P. S. Gurel, A. L. Hatch, H. N. Higgs, Connecting the cytoskeleton to the endoplasmic reticulum and Golgi. *Curr. Biol.* **24**, R660–R672 (2014).
72. D. Zhang, Interplay between endoplasmic reticulum membrane contacts and actomyosin cytoskeleton. *Cytoskeleton (Hoboken)* **77**, 241–248 (2020).
73. X. A. Cui, H. Zhang, A. F. Palazzo, p180 promotes the ribosome-independent localization of a subset of mRNA to the endoplasmic reticulum. *PLoS Biol.* **10**, e1001336 (2012).
74. J. Hu *et al.*, High stretchability, strength, and toughness of living cells enabled by hyperelastic vimentin intermediate filaments. *Proc. Natl. Acad. Sci. U.S.A.* **116**, 17175–17180 (2019).